INT. J. BIOAUTOMATION, 2021, 25(3), 249-270 doi: 10.7546/ijba.2021.25.3.000781

# Parallel Distributed Framework for State Space Adaptive Filter for Removal of PLI from Cardiac Signals

**Inam ur Rehman[1*], Hasan Raza[2], Nauman Razzaq[3], Tahir Zaidi[1]**

[1]*Department of Electrical Engineering*
*College of Electrical and Mechanical Engineering*
*National University of Science and Technology (NUST), Islamabad, Pakistan*
*E-mails: muhammad.inam@ceme.nust.edu.pk, tahirzaidi@ceme.nust.edu.pk*

[2]*Department of Electrical Engineering*
*Hamdard Institute of Engineering and Technology*
*Hamdard University Islamabad Campus (HUIC), Islamabad, Pakistan*
*E-mail: hasan.raza@hamdard.edu.pk*

[3]*Department of Electrical Engineering*
*National University of Technology*
*Islamabad, Pakistan*
*E-mail: nauman.razzaq@nutech.edu.pk*

[*]*Corresponding author*

**Received: April 27, 2020** **Accepted: November 20, 2020**

**Published: September 30, 2021**

***Abstract:*** *Cardiac signals are often corrupted by artefacts like power line interference (PLI) which may mislead the cardiologists to correctly diagnose the critical cardiac diseases. The cardiac signals like high resolution electrocardiogram (HRECG), ultra-high frequency ECG (UHF-ECG) and intracardiac electrograms are the specialized techniques in which higher frequency component of interest up to 1 KHz are observed. Therefore, a state space recursive least square (SSRLS) adaptive algorithm is applied for the removal of PLI and its harmonics. The SSRLS algorithm is an effective approach which extracts the desired cardiac signals from the observed signal without any need of reference signal. However, SSRLS is inherited computational heavy algorithm; therefore, filtration of increased number of PLI harmonics bestow an adverse impact on the execution time of the algorithm. In this paper, a parallel distributed SSRLS (PD-SSRLS) algorithm is introduced which runs the computationally expensive SSRLS adaptive algorithm parallelly. The proposed architecture efficiently removes the PLI along with its harmonics even the time alignment among the contributing nodes is not the same. Furthermore, the proposed PD-SSRLS scheme provides less computational cost as compared to sequentially operated SSRLS algorithm. A comparison has been drawn between the proposed PD-SSRLS algorithm and sequentially operated SSRLS algorithm in term of qualitative and quantitative performances. The simulation results show that the proposed PD-SSRLS architecture provides almost same qualitative and quantitative performances than that of sequentially operated SSRLS algorithm with less computational cost.*

***Keywords:*** *Adaptive noise cancellation, Cardiac signal processing, PD-SSRLS, Power line interference, State space adaptive filter.*

## Introduction

From the last two-decades, cardiac signal processing plays vital role for the diagnosis and prognosis of major critical heart ailments like cardiac ischemia, cardiomyopathies, myocardial ischemia and infarction, sudden cardiac death (SCD), atrial and ventricular abnormalities, ventricular electrical dyssynchrony (e-DYS), pericarditis and heart rate variability (HRV), etc., [5, 8, 24]. However, due to multifaceted morphology and nonstationary nature of abnormal cardiac signals, most of cardiologists are still struggling to precisely recognize explicit biological markers and fiducial points under observational noise. Advancement in innovative technology leads to acquire high resolution electrocardiogram (HRECG) with bandwidth upto

500 Hz and ultra-high frequency ECG (UHF-ECG) having frequency upto 1000 Hz both are used for prognosis of SCD and e-DYS, respectively [10, 15, 16, 27, 32]. Therefore, due to wider bandwidth of cardiac signal like; HRECG, UHF-ECG as compared to standard ECG signal (0-80 Hz), the cardiac signal becomes more susceptible to Power line Interference (PLI) as an external noises. On the other hand, the cables in cardiac monitoring room which carry cardiac signals are prone to electromagnetic interference (EMI) due to main power supply lines or sockets and this factor cannot be evaded completely even if the device has very high common mode rejection; likewise, PLI frequency (50 Hz or 60 Hz) and its harmonics overlapping with the useful spectrum of cardiac signal, overwhelms tiny features that may be critical for clinical monitoring and diagnosis. Therefore, removal of such PLI signal without effecting the underlying cardiac activity becomes a challenging task.

Various approaches have been introduced in literature to remove PLI noise from the observed cardiac signals [6, 28, 29, 34, 42–44]. Among these approaches, notch filtering is one of the most simple and conventional technique to remove PLI noise from the observed cardiac signals [29, 34, 42]. The notch filter uses the infinite impulse response (IIR) filter which provides smaller filter order as compared to finite impulse response (FIR) filter, but it causes the nonlinear phase distortion [6, 28, 43, 44]. Furthermore, the notch filter may remove the underlying cardiac signal components along with PLI, which could mislead the results especially in case of aforementioned critical diseases.

Various other approaches which are used for cardiac signal denoising are based on signal decomposition techniques, e.g., empirical mode decomposition (EMD) [38, 39], eigen value decomposition (EVD) [14] and Fourier decomposition method [4, 19, 36, 37]. In EMD and its modified algorithms [1, 30], the observational noise is decomposed into different levels of detail coefficients called intrinsic mode functions (IMFs). Therefore, removing of baseline wander (BW) and PLI noise means setting these IMFs to zero which leads to loss of significant underlying cardiac activity. Likewise, in EVD [35], the estimated observational noise eigenvectors are removed simultaneously which also eradicate some critical features of cardiac signals. On the other hand, in Fourier decomposition method the signal is decomposed into different frequency bands [40]. However, for removal of PLI noise, the complete band is removed which bestow a critical impact on the acquisition of desired signal. The subtraction procedure also efficiently removes the PLI noise from cardiac signal and it even handles the drifts in amplitude and frequency of PLI interference signal very well [20, 25, 26].

To overcome such problem, adaptive filtration techniques have been introduced in the literature to better handle and retain the underlying cardiac activity intact [11, 13]. In this context, Widrow et al. [45] introduced the concept of adaptive noise cancellation (ANC) and Glover [9] applied ANC for PLI removal by adaptively tracking of PLI sinusoids with known parameters like amplitude, phase and frequency. Later on, authors in [23] modified ANC technique for two unknown parameters like amplitude and phase of PLI signal while the frequency is known. Likewise, Satija et al. [33] modified ANC algorithm for all three unknown parameters. Therefore, the ANC approaches need of reference signal, makes medical devices expensive. To overcome the problem related to the acquisition of reference signal, authors in [2, 3, 18] implemented ANC without sampling reference signal for eliminating PLI noise. Moreover, authors in [31] introduced state space recursive least square (SSRLS) filtering algorithm which provides fast convergence performance as compared to gradient and recursive based adaptive algorithm. The SSRLS algorithm effectively handles the frequency drifts and removes the PLI and its harmonics for HRECG signal (upto 500 Hz) on behalf of higher computational cost.

The computational cost of SSRLS algorithm significantly increases with the increase in number of harmonics which provides a critical impact on its real time implementation.

In this paper, the scope of [32] is extended by making it feasible for HRECG signal and UHF-ECG signal having frequency components up to 500 Hz and 1000 Hz, respectively. For these cardiac signals, one needs to filter out the fundamental component of PLI and its harmonics up to 500 Hz and 1000 Hz which are present in the observed signals. In this context, the parallel distributed SSRLS (PD-SSRLS) architecture is introduced. The proposed architecture runs the SSRLS algorithm in parallel fashion using non-aligned time indexes. The proposed PD-SSRLS algorithm provides less computational cost with almost same performance as compared to sequentially operated SSRLS algorithm.

## Materials and methods

### *State space model of PLI*

When the cardiac signal is corrupted by PLI signal at time instant $n$ can be modeled as:

$$y[n] = x_{clean}[n] + I[n], \tag{1}$$

where $y[n]$ is the contaminated signal, $x_{clean}[n]$ is pure cardiac signal and $I[n]$ is the PLI signal which can be defined as:

$$I[n] = \sum_{i=1}^{M} a_i sin(2\pi f i \Delta T n + \theta_i), \tag{2}$$

where $M$ shows the total number of harmonics of PLI signal, $a_i$ is the amplitude of $i^{th}$ harmonic component, $f$ is fundamental frequency component, $\Delta T$ is the sampling period and $\theta_i$ is the phase of $i^{th}$ harmonic. The PLI signal for fundamental frequency at $i = 1$ can be expressed as:

$$I[n] = a_1 sin(\omega n + \theta_1), \tag{3}$$

where $\omega = 2\pi f \Delta T$ is the frequency in rad/sec. The state space representation of PLI model of $1^{st}$ harmonic given in Eq. (3) has two states which can be written as:

$$\begin{aligned} x_1[n] &= a_1 sin(\omega n + \theta_1), \\ x_2[n] &= a_1 sin(\omega n + \theta_1 + \pi/2) = a_1 cos(\omega n + \theta_1). \end{aligned} \tag{4}$$

With the help of trigonometric identities, the Eq. (4) can be rewritten as:

$$\begin{aligned} x_1[n] &= a_1 sin(\omega n)cos(\theta_1) + a_1 cos(\omega n)sin(\theta_1), \\ x_2[n] &= a_1 cos(\omega n)cos(\theta_1) - a_1 sin(\omega n)sin(\theta_1). \end{aligned} \tag{5}$$

Rewrite Eq. (5) in matrix form, we get

$$\begin{bmatrix} x_1[n] \\ x_2[n] \end{bmatrix} = \begin{bmatrix} cos(\omega n) & sin(\omega n) \\ -sin(\omega n) & cos(\omega n) \end{bmatrix} \begin{bmatrix} a_1 sin(\theta_1) \\ a_1 cos(\theta_1) \end{bmatrix}. \tag{6}$$

The initial conditions at $n = 0$, Eq. (6) can be expressed as:

$$\begin{aligned} x_1[0] &= a_1 sin(\theta_1), \\ x_2[0] &= a_1 cos(\theta_1). \end{aligned} \tag{7}$$

Putting the initial conditions as defined in Eq. (7) into Eq. (6) at $k = 0$, we have

$$\begin{bmatrix} x_1[1] \\ x_2[1] \end{bmatrix} = \begin{bmatrix} cos\omega & sin\omega \\ -sin\omega & cos\omega \end{bmatrix} \begin{bmatrix} x_1[0] \\ x_2[0] \end{bmatrix}. \tag{8}$$

Likewise, the generalized form for $n > 1$ can be expressed as:

$$\begin{bmatrix} x_1[n+1] \\ x_2[n+1] \end{bmatrix} = \begin{bmatrix} cos\omega & sin\omega \\ -sin\omega & cos\omega \end{bmatrix} \begin{bmatrix} x_1[n] \\ x_2[n] \end{bmatrix}. \tag{9}$$

Ideally, the main power lines comprise only fundamental frequency component of 50 or 60 Hz (depends on the regional area). However, in practical situation the integer multiple of fundamental frequency component called harmonics are also present. Due to half wave symmetry property the power line system has only odd harmonics [7]. Therefore, the generalized PLI state space model for $M$ harmonics can be expressed in (10):

$$\begin{bmatrix} x_1[n+1] \\ x_2[n+1] \\ \vdots \\ x_{2M-1}[n+1] \\ x_{2M}[n+1] \end{bmatrix} = \begin{bmatrix} cos\omega & sin\omega & \cdots & 0 \\ -sin\omega & cos\omega & \cdots & 0 \\ \vdots & \vdots & \ddots & \vdots \\ 0 & \cdots & cosM\omega & sinM\omega \\ 0 & \cdots & -sinM\omega & cosM\omega \end{bmatrix} \begin{bmatrix} x_1[n] \\ x_2[n] \\ \vdots \\ x_{2M-1}[n] \\ x_{2M}[n] \end{bmatrix}. \tag{10}$$

## *Proposed methodology*

### *SSRLS algorithm*

The SSRLS adaptive algorithm is based on state space model which provides good tracking capability with high accuracy [22,31]. The unforced discrete time state space model for removal of PLI noise using SSRLS adaptive filter can be written as:

$$\begin{aligned} \mathbf{x}[n+1] &= \mathbf{A}\mathbf{x}[n], \\ y[n] &= \mathbf{c}\mathbf{x}[n] + v[n], \end{aligned} \tag{11}$$

where $\mathbf{x}[n]$ is a state vector at time index $n$, $y[n]$ is the observed output, $v[n]$ is the observation noise, $\mathbf{A}$ shows the state transition matrix which should be invertible and $\mathbf{c}$ is output vector that should be full rank and their pair $(\mathbf{A}, \mathbf{c})$ is assumed to be $l$-step observable [22]. The predicted state $\bar{\mathbf{x}}[n]$ which is based on the *a priori* estimated state $\hat{\mathbf{x}}[n-1]$ can be defined as:

$$\bar{\mathbf{x}}[n] = \mathbf{A}\hat{\mathbf{x}}[n-1]. \tag{12}$$

Similarly, the predicted output $\bar{y}[n]$ and the prediction error $\varepsilon[n]$ can be defined as:

$$\begin{aligned} \bar{y}[n] &= \mathbf{c}\bar{\mathbf{x}}[n], \\ \varepsilon[n] &= y[n] - \bar{y}[n]. \end{aligned} \tag{13}$$

The SSRLS is a recursive algorithm which recursively estimates the state $\hat{\mathbf{x}}[n]$ given that the prior estimated state $\hat{\mathbf{x}}[n-1]$ on advent of observation $y[n]$. The SSRLS adaptive algorithm updates the states and can be expressed as [22]:

$$\hat{\mathbf{x}}[n] = \bar{\mathbf{x}}[n] + \mathbf{k}[n]\varepsilon[n], \tag{14}$$

where $\mathbf{k}[n]$ is the observational gain. Likewise, estimated output $\hat{y}[n]$ and the estimated error $e[n]$ can be defined as:

$$\begin{aligned} \hat{y}[n] &= \mathbf{c}\hat{\mathbf{x}}[n], \\ e[n] &= y[n] - \hat{y}[n]. \end{aligned} \tag{15}$$

The observational gain which can be determined through least square method can be expressed as:

$$\mathbf{k}[n] = \mathbf{\Phi}^{-1}[n]\mathbf{c}^{\mathrm{T}}, \tag{16}$$

where $\Phi[n]$ is autocorrelation matrix and it can be written in form of recursively updated difference Lyapunov equation as:

$$\mathbf{\Phi}[n] = \lambda \mathbf{A}^{-\mathrm{T}}\mathbf{\Phi}[n-1]\mathbf{A}^{-1} + \mathbf{c}^{\mathrm{T}}\mathbf{c}, \tag{17}$$

where $0 < \lambda < 1$ is the forgetting factor which controls the rate of convergence of adaptive filter. With the help of matrix inversion lemma and some algebraic manipulation the inverse of $\mathbf{\Phi}^{-1}[n]$ can become the Riccati equation as [12]:

$$\begin{aligned} \mathbf{\Phi}^{-1}[n] = {} & \lambda^{-1}\mathbf{A}\mathbf{\Phi}^{-1}[n-1]\mathbf{A}^{\mathrm{T}} - \lambda^{-2}\mathbf{A}\mathbf{\Phi}^{-1}[n-1]\mathbf{A}^{\mathrm{T}}\mathbf{c}^{\mathrm{T}} \times \\ & \times [I + \lambda^{-1}\mathbf{c}\mathbf{A}\mathbf{\Phi}^{-1}[n-1]\mathbf{A}^{\mathrm{T}}\mathbf{c}^{\mathrm{T}}]^{-1}\mathbf{c}\mathbf{A}\mathbf{\Phi}^{-1}[n-1]\mathbf{A}^{\mathrm{T}}. \end{aligned} \tag{18}$$

Finally, the state space representation of sequentially operated SSRLS can be expressed as [22]:

$$\begin{aligned} \mathbf{w}[n+1] &= \lambda \mathbf{A}^{-\mathrm{T}}\mathbf{w}[n] + \mathbf{c}^{\mathrm{T}}y[n], \\ \hat{\mathbf{x}}[n] &= \lambda \mathbf{\Phi}^{-1}[n]\mathbf{A}^{-\mathrm{T}}\mathbf{w}[n] + \mathbf{k}[n]y[n], \end{aligned} \tag{19}$$

where $\mathbf{w}[n]$ is the process state vector, $y[n]$ is the input to the system, $\hat{\mathbf{x}}[n]$ is the output and the quadruplet $(\lambda\mathbf{A}^{-\mathrm{T}}, \mathbf{c}^{\mathrm{T}}, \lambda\mathbf{\Phi}^{-1}[n]\mathbf{A}^{-\mathrm{T}}, \mathbf{k}[n])$ represent the state space matrices.The flow diagram of sequentially operated SSRLS algorithm is shown in Fig. 1.

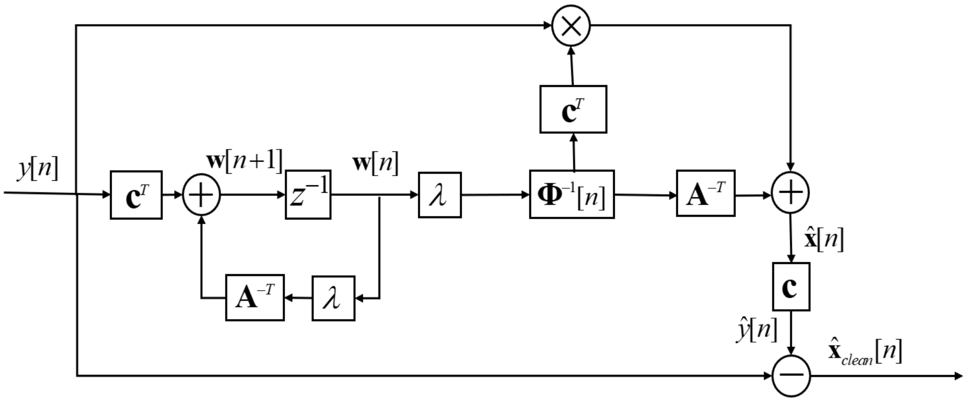


Fig. 1 Working of SSRLS adaptive filter in sequential form

Table 1. SSRLS adaptive filter

| |
|---|
| Initialize: $\mathbf{w}[n]$, $\lambda$, $\mathbf{k}[n-1]$, $\mathbf{\Phi}[n-1]$ |
| $\mathbf{w}[n+1] = \lambda \mathbf{A}^{-\mathrm{T}}\mathbf{w}[n] + \mathbf{c}^{\mathrm{T}} y[n]$ |
| $\hat{\mathbf{x}}[n] = \lambda \mathbf{\Phi}^{-1}[n]\mathbf{A}^{-\mathrm{T}}\mathbf{w}[n] + \mathbf{k}[n]y[n]$ |
| $\mathbf{k}[n] = \mathbf{\Phi}^{-1}[n]\mathbf{c}^{\mathrm{T}}$ |
| $\mathbf{\Phi}^{-1}[n] = \lambda^{-1}\mathbf{A}\mathbf{\Phi}^{-1}[n-1]\mathbf{A}^{\mathrm{T}} \times$ |
| $\times \lambda^{-2}\mathbf{A}\mathbf{\Phi}^{-1}[n-1]\mathbf{A}^{\mathrm{T}}\mathbf{c}^{\mathrm{T}} \times$ |
| $\times [I + \lambda^{-1}\mathbf{c}\mathbf{A}\mathbf{\Phi}^{-1}[n-1]\mathbf{A}^{\mathrm{T}}\mathbf{c}^{\mathrm{T}}]^{-1} \times$ |
| $\times \mathbf{c}\mathbf{A}\mathbf{\Phi}^{-1}[n-1]\mathbf{A}^{\mathrm{T}}$ |

The estimated noise free cardiac signals $\hat{x}_{clean}[n]$ can be obtained by taking the difference of estimated output signal $\hat{y}[n]$ and the contaminated cardiac signal $y[n]$, which can be written as:

$$\hat{x}_{clean}[n] = y[n] - \hat{y}[n]. \tag{20}$$

Likewise, the summarized form of sequentially operated SSRLS adaptive filter algorithm is shown in Table 1.

*Proposed parallel distributed system model*

In conventional SSRLS algorithm, all filter parts are interdependent on each other which makes the algorithm to run in cascade fashion. However, in proposed PD-SSRLS algorithm, all filter parts are capable to work in parallel fashion and this has been done by putting time non-alignment among the parts of the algorithm. While setting the time non-alignment among the participating parts of the algorithm, it must be noted that the behavior of the filter is not uncertain while it is implemented on desired application, secondly, all the filter parts are able to operate in parallel fashion. The flow diagram of proposed PD-SSRLS is depicted in Fig 2, which consists on four processing nodes, i.e., $N_1$, $N_2$, $N_3$ and, $N_4$.

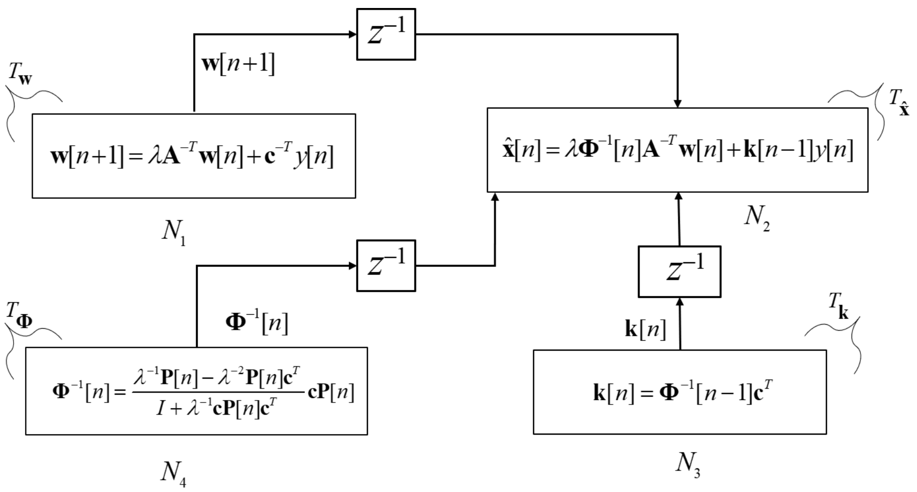


Fig. 2 Proposed parallel distributed architecture

The notation "$T_{\mathbf{x}}$" represents the processing time used in processing node $\mathbf{x}$. The processing time taken by the nodes $N_1$, $N_2$, $N_3$ and $N_4$ are based on the process states $\mathbf{w}_n$, estimated output $\hat{\mathbf{x}}_n$, the observation gain $\mathbf{k}_n$, the autocorrelation matrix $\mathbf{\Phi}_n$, be $T_{\mathbf{w}}$, $T_{\hat{\mathbf{x}}}$, $T_{\mathbf{k}}$, $T_{\mathbf{\Phi}}$, respectively.

Consequently, the overall time required by SSRLS algorithm when it operates sequentially can be written as:

$$T_{tot} = T_{\mathbf{w}} + T_{\hat{\mathbf{x}}} + T_{\mathbf{k}} + T_{\mathbf{\Phi}}. \tag{21}$$

Here $T_{\mathbf{\Phi}}$ is the maximum contributor in overall processing time, the strict and sufficient condition based on multiplication and addition computations with respect to fast convergence performance can be defined as:

$$T_{\mathbf{w}}, T_{\hat{\mathbf{x}}}, T_{\mathbf{k}} \leq T_{\mathbf{\Phi}}. \tag{22}$$

The mismatch factor $\xi$ between the aligned and nonaligned time indexes can be defined as:

$$\xi = \|\varepsilon_{seq} - \varepsilon_{NA}\|, \tag{23}$$

where $\varepsilon_{seq}$ and $\varepsilon_{NA}$ are the errors based on sequentially operated SSRLS algorithm and proposed PD-SSRLS algorithm, respectively.

*Computational complexity*
The computational cost of an algorithm provides significant importance particularly in real-time applications. In this section, the complexity comparison of sequentially and parallel operated SSRLS algorithms are discussed. The complexity of state space representation of sequentially operated SSRLS algorithm as mentioned in Eq. (19) is given in Table 2; while, Table 3 furnishes the complexity of Eqs. (16) and (18), respectively. In the sequentially operated SSRLS adaptive filter based on Eqs. (16), (18) and (19) requires $2n^3 + 9n^2 + 5n$ multiplications and $2n^3 + 5n^2 - 4n + 1$ additions per iteration, where $n$ shows the system order.

The proposed PD-SSRLS architecture shows less computational cost as compared to sequentially operated SSRLS algorithm. The proposed algorithm requires parallely $2n^3 + 5n^2 + 2n$ multiplications and $2n^3 + n^2 - 2n + 1$ additions per iteration at maximum. However, in case of sequentially operated SSRLS adaptive filter, the node $N_3$ based on $\Phi[n]$ provides the maximum computational cost as compared to other nodes is presented in Table 3. The summarized form of complexity comparison between sequentially operated SSRLS and proposed PD-SSRLS algorithms is presented in Table 4. It can be seen that the proposed architecture provides reduced complexity as compared to sequentially operated SSRLS algorithm.

*Performance parameters*
Besides the visual inspection, a quantitative measures for the efficiency of the filtering methods and the clinical acceptability of the reconstructed signal both are employed to provide accurate accessions on the proposed approach. Consequently, four performance evaluation indexes are employed to compare the original (noise-free) cardiac signal with the filtered signal. Therefore, among of these performance metrics, the suppression ratio can be written as [21]:

$$\gamma = 10\log_{10}\left\{\frac{\|\mathbf{y}\|_2^2}{\|\hat{\mathbf{x}}_{clean}\|_2^2}\right\}, \tag{24}$$

where $\mathbf{y}$ is the contaminated cardiac signal and $\hat{\mathbf{x}}_{clean}$ is the filtered signal. In case of highly corrupted cardiac signal (low input SNR), the value of suppression ratio $\gamma$ should be observed as high as possible.

Table 2. Computational complexity of Eq. (19)

| Eq.# | Operation | Multiplications | Additions/ Subtractions | Division |
|---|---|---|---|---|
| * | $\mathbf{d}_{n\times 1} = \lambda_{1\times 1}\mathbf{A}_{n\times n}\mathbf{w}[n]_{n\times 1}$ | $n^2$ | $n^2 - n$ | – |
| | $\mathbf{e}_{n\times 1} = \mathbf{c}^T[n]_{n\times 1}y[n]_{1\times 1}$ | $n$ | – | – |
| (19a) | $\mathbf{w}[n+1]_{n\times 1} = \mathbf{d}_{n\times 1} + \mathbf{e}_{n\times 1}$ | – | $n$ | – |
| | | $n^2 + n$ | $n^2$ | – |
| | $\mathbf{f}_{n\times 1} = \mathbf{n}[n]_{n\times 1}y[n]_{1\times 1}$ | $n$ | – | – |
| | $\mathbf{g}_{n\times 1} = \mathbf{A}^{-T}_{n\times n}\mathbf{w}[n]_{n\times 1}$ | $n^2$ | $n^2 - n$ | – |
| | $\mathbf{h}_{n\times 1} = \lambda_{1\times 1}\mathbf{\Phi}^{-1}[n]_{n\times n}\mathbf{g}_{n\times 1}$ | $n^2 + n$ | $n^2 - n$ | – |
| (19b) | $\hat{\mathbf{x}}[n]_{n\times 1} = \mathbf{h}_{n\times 1} + \mathbf{f}_{n\times 1}$ | – | $n$ | – |
| | | $2n^2 + 2n$ | $2n^2 - n$ | – |
| | Grand total | $3n^2 + 3n$ | $3n^2 - n$ | – |

* $\lambda_{1\times 1}\mathbf{A}_{n\times n}$ computed offline

Table 3. Computational complexity of Eqs. (16) and (18)

| Eq.# | Operation | Multiplications | Additions/ Subtractions | Division |
|---|---|---|---|---|
| (16) | $\mathbf{n}[n]_{n\times 1} = \mathbf{\Phi}^{-1}[n]_{n\times n}\mathbf{c}^T[n]_{n\times 1}$ | $n^2$ | $n^2 - n$ | – |
| | $\mathbf{P}_{n\times n} = \mathbf{A}_{n\times n}\mathbf{\Phi}^{-1}[n-1]_{n\times n}\mathbf{A}^T_{n\times n}$ | $2n^3$ | $2n^3 - 2n^2$ | – |
| | $\mathbf{Q}_{n\times n} = \lambda^{-1}_{1\times 1}\mathbf{P}_{n\times n}$ | $n^2$ | – | – |
| | $\mathbf{r}_{n\times 1} = \mathbf{Q}_{n\times n}\mathbf{c}^T[n]_{n\times 1}$ | $n^2$ | $n^2 - n$ | – |
| | $\mathbf{s}_{1\times n} = \mathbf{c}[n]_{1\times n}\mathbf{P}_{n\times n}$ | $n^2$ | $n^2 - n$ | – |
| | $t_{1\times 1} = \mathbf{c}[n]_{1\times n}\mathbf{r}_{n\times 1}$ | $n$ | – | – |
| | $u_{1\times 1} = I_{1\times 1} + t_{1\times 1}$ | – | 1 | – |
| | $v_{1\times 1} = u^{-1}_{1\times 1}$ | – | – | 1 |
| | $\mathbf{l}_{1\times n} = v_{1\times 1}\mathbf{s}_{1\times n}$ | $n$ | – | – |
| | $\mathbf{M}_{n\times n} = \lambda_{1\times 1}\mathbf{r}_{n\times 1}\mathbf{l}_{1\times n}$ | $2n^2$ | – | – |
| (18) | $\mathbf{\Phi}^{-1}[n]_{n\times n} = \mathbf{Q}_{n\times n} - \mathbf{M}_{n\times n}$ | – | $n^2$ | – |
| | Total | $2n^3 + 5n^2 + 2n$ | $2n^3 + n^2 - 2n + 1$ | 1 |
| | Grand total | $2n^3 + 6n^2 + 2n$ | $2n^3 + 2n^2 - 3n + 1$ | 1 |

Table 4. Comparison of computational complexity

| Algorithm | Multiplications | Additions/Subtractions | Division |
|---|---|---|---|
| Sequentially operated SSRLS | $2n^3 + 9n^2 + 5n$ | $2n^3 + 5n^2 - 4n + 1$ | 1 |
| Proposed PD-SSRLS | $2n^3 + 5n^2 + 2n$ | $2n^3 + n^2 - 2n + 1$ | 1 |

Secondly, the Pearson's correlation coefficient is computed which can be expressed as [41]:

$$\rho = \frac{E\left[\mathbf{x}_{clean}\hat{\mathbf{x}}_{clean}\right]}{\sigma_{\mathbf{x}_{clean}}\sigma_{\hat{\mathbf{x}}_{clean}}}, \tag{25}$$

where $\sigma_{\mathbf{x}_{clean}}$ and $\sigma_{\hat{\mathbf{x}}_{clean}}$ both are the standard deviation of pure noise-free cardiac signal and denoised signal, respectively.The value of correlation coefficient shows the shape similarity of the filtered signals to original noise-free cardiac signals. The $E[\cdot]$ operator is the expectation operator and can de defined as:

$$E(x) = \sum xp(x),$$

where $p(x)$ is the probability of discrete time random variable.

Furthermore, the well known SNR and mean square error (MSE) are expressed as [4]:

$$SNR_{out} = 10\log_{10}\left\{\frac{\sigma^2_{\mathbf{x}_{clean}}}{\sigma^2_{(\mathbf{x}_{clean}-\hat{\mathbf{x}}_{clean})}}\right\}, \tag{26}$$

$$MSE = \frac{1}{N}\sum_{n=1}^{N}(x_{clean}[n] - \hat{x}_{clean}[n])^2, \tag{27}$$

where $x[n]$ is the pure noise-free cardiac signal. The output SNR should be high because the remaining interference should be as low as possible. On the other hand, the MSE defines how closer is the recovered signal to the clean signal.

## Results and discussions

In this section, both the qualitative and quantitative based results are presented. The proposed PD-SSRLS algorithm is then compared with the sequentially operated SSRLS adaptive filter. To substantiate the validation of proposed algorithm, three types of cardiac signals are used in this study, i.e., HRECG, UHF-ECG and IEGM. The HRECG and atrial IEGM signals both are acquired from National Institute of Heart Diseases (NIHD) having sampling rate of 1000 samples/s and 2000 samples/s, respectively. While UHF-ECG signal used in this paper is provided by Dr. Pavel Jurak having sampling rate of 5000 samples/s [16].

### *Qualitative performance*

The normalized two second segment of pure HRECG signal and its frequency spectrum are shown in Fig. 3. In Fig. 3(b), the frequency spectrum shows that the recorded HRECG signal has no PLI component and its harmonics however, it contains high frequency contents. Removal of these high frequency contents is not within the scope of this paper and the existence of these high frequency contents does not affect the performance of the proposed architecture.

To validate the qualitative performance of proposed algorithm, the PLI noise having fundamental frequency of 50 Hz and its next four odd harmonics are considered. The normalized magnitude of 1$^{st}$, 3$^{rd}$, 5$^{th}$, 7$^{th}$ and 9$^{th}$ harmonic components along with composite PLI signal is shown in Fig. 4. Furthermore, the contaminated HRECG signal having SNR value of 3 dB is shown in Fig. 5. The PLI contaminated HRECG signal is the mixture of compound PLI signal and pure HRECG signal. On the other hand, the frequency spectrum of contaminated HRECG clearly depicts the harmonics as an odd integer multiple of 50 Hz are illustrated in Fig. 5(b).

For PLI signal having five harmonic components (including fundamental) the system matrix $\mathbf{A}$ entail the dimensions of $10 \times 10$. Likewise, the state vector $\mathbf{w}$ requires $10 \times 1$ and the observational vector $\mathbf{c}$ entails $1 \times 10$. For tracking of 1$^{st}$, 3$^{rd}$, 5$^{th}$, 7$^{th}$ and 9$^{th}$ harmonics of PLI, the $\mathbf{c}$ vector in (15) can be chosen as:

$$\mathbf{c} = \begin{bmatrix} 1 & 0 & 1 & 0 & 1 & 0 & 1 & 0 & 1 & 0 \end{bmatrix}. \tag{28}$$

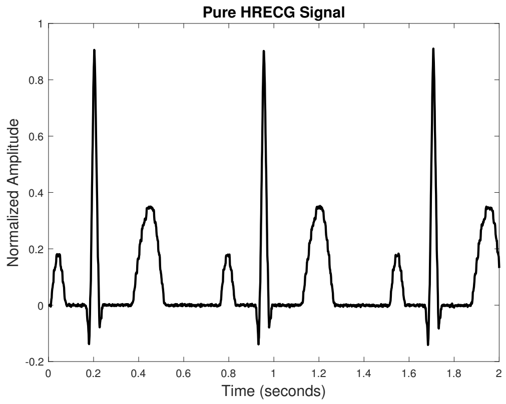


(a) Pure HRECG signal

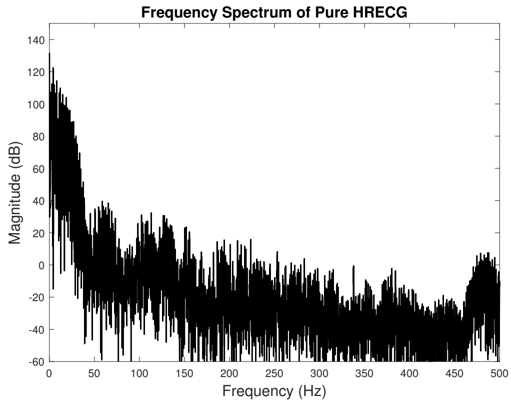


(b) Frequency response

Fig. 3 Pure HRECG signal with sampling rate 1000 samples/s and its frequency spectrum

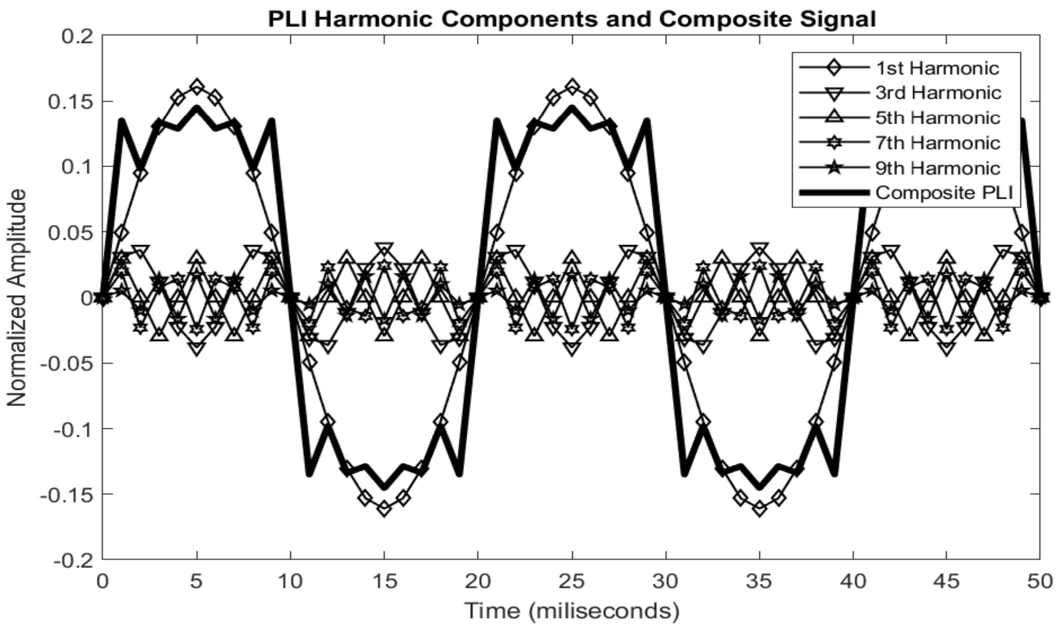


Fig. 4 The amplitude scale of odd harmonics in composite PLI signal

The SSRLS adaptive filter updates the states based on recursive approach; therefore, initialization of the parameters like $\lambda$, $\hat{\mathbf{x}}[0]$, $\mathbf{\Phi}^{-1}[0]$, and $\mathbf{n}[0]$ are required. For the simulation purpose, these parameters are initialized as $\lambda = 0.9999$, $\hat{\mathbf{x}}[0] = [0\ 0\ 0\ 0\ 0\ 0\ 0\ 0\ 0\ 0]^{\mathrm{T}}$ and

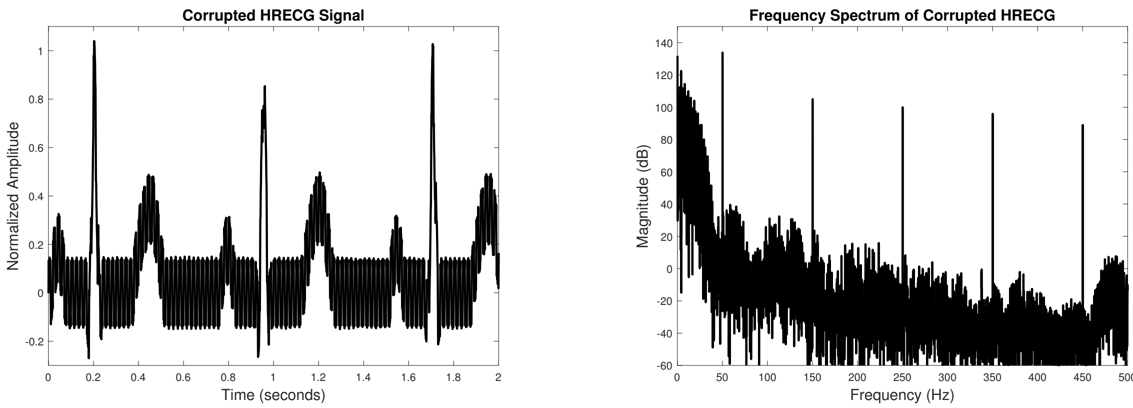


(a) PLI corrupted HRECG (b) Frequency Response of corrupted HRECG

Fig. 5 The contaminated HRECG signal with fundamental component and odd harmonics of PLI interference and its frequency spectrum

$\mathbf{\Phi}^{-1}[0] = \delta I + \mathbf{c}\mathbf{c}^{\mathrm{T}}$, where $\delta$ is taken as 0.1 and $\mathbf{\Phi}^{-1}[0]$ can be represented as:

$$\begin{bmatrix} 0.1 & 0 & 0 & 0 & 0 & 0 & 0 & 0 & 0 & 0 \\ 0 & 0.1 & 0 & 0 & 0 & 0 & 0 & 0 & 0 & 0 \\ 0 & 0 & 0.1 & 0 & 0 & 0 & 0 & 0 & 0 & 0 \\ 0 & 0 & 0 & 0.1 & 0 & 0 & 0 & 0 & 0 & 0 \\ 0 & 0 & 0 & 0 & 0.1 & 0 & 0 & 0 & 0 & 0 \\ 0 & 0 & 0 & 0 & 0 & 0.1 & 0 & 0 & 0 & 0 \\ 0 & 0 & 0 & 0 & 0 & 0 & 0.1 & 0 & 0 & 0 \\ 0 & 0 & 0 & 0 & 0 & 0 & 0 & 0.1 & 0 & 0 \\ 0 & 0 & 0 & 0 & 0 & 0 & 0 & 0 & 0.1 & 0 \\ 0 & 0 & 0 & 0 & 0 & 0 & 0 & 0 & 0 & 0.1 \end{bmatrix}.$$

The initial observer gain $\mathbf{k}[0]$ can be identified by using $\mathbf{\Phi}^{-1}[0]$. The frequency spectrum of adaptively tracking of PLI signal by using proposed PD-SSRLS architecture is shown in Fig. 6. It can be seen that the proposed architecture provides good tracking for all these five harmonics components (including fundamental) of PLI signal.

Furthermore, a 10 seconds segment of pure and contaminated HRECG signal is shown in Fig. 7. It can be observed that the proposed PD-SSRLS architecture provides the same tracking performance as compared to SSRLS algorithm.

Likewise, UHF-ECG and IEGM based clean and corrupted with PLI signals are shown in Fig. 8 and Fig. 9, respectively. It can be observed that the proposed architecture provides the same tracking performance than that of sequentially operated SSRLS algorithm.

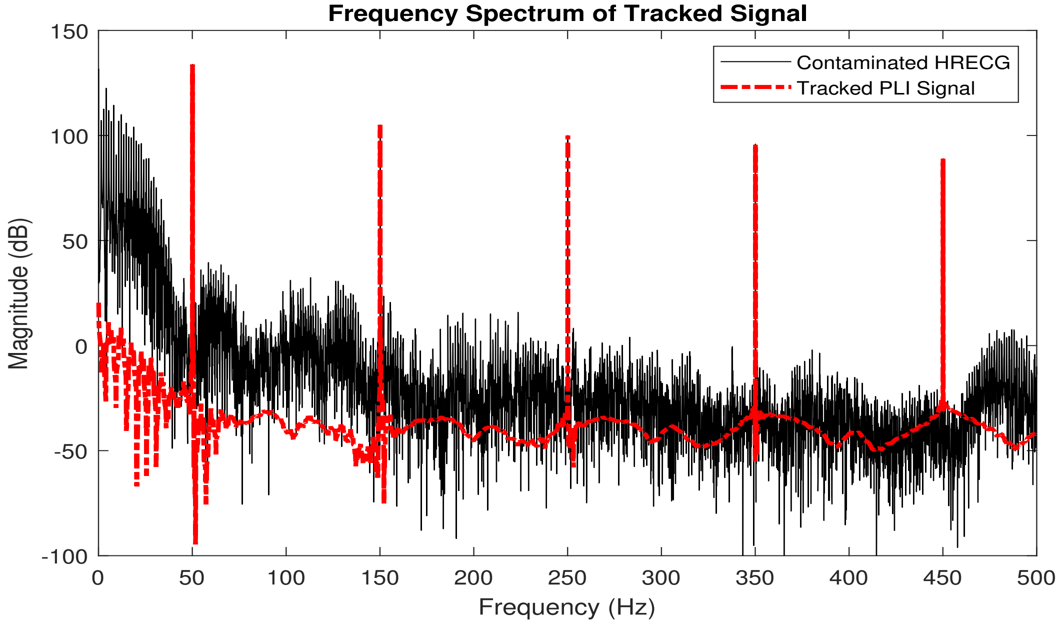


Fig. 6 Frequency spectrum of tracked PLI signal

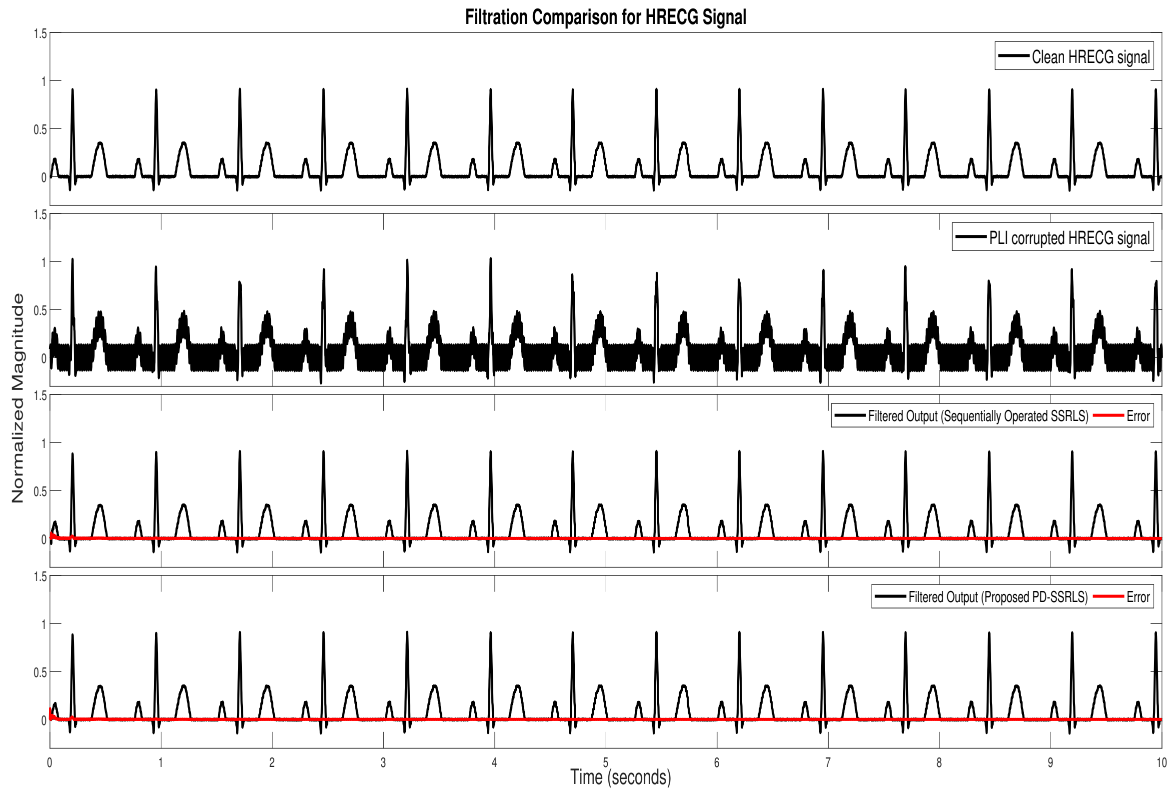


Fig. 7 Filtration comparison between Proposed PD-SSRLS and sequentially-operated SSRLS for HRECG signal

Furthermore, Fig. 10 shows the PLI corrupted HRECG signal with abrupt and linear change in amplitude. It can be realized that both the proposed PD-SSRLS and sequentially-operated SSRLS algorithms take approximately 500 ms to track the abrupt deviation in amplitude of PLI signal and provides same convergence performance in case of linear deviation in amplitude of PLI interference signal.


Fig. 8 Filtration comparison between Proposed PD-SSRLS and sequentially-operated SSRLS for UHF-ECG signal

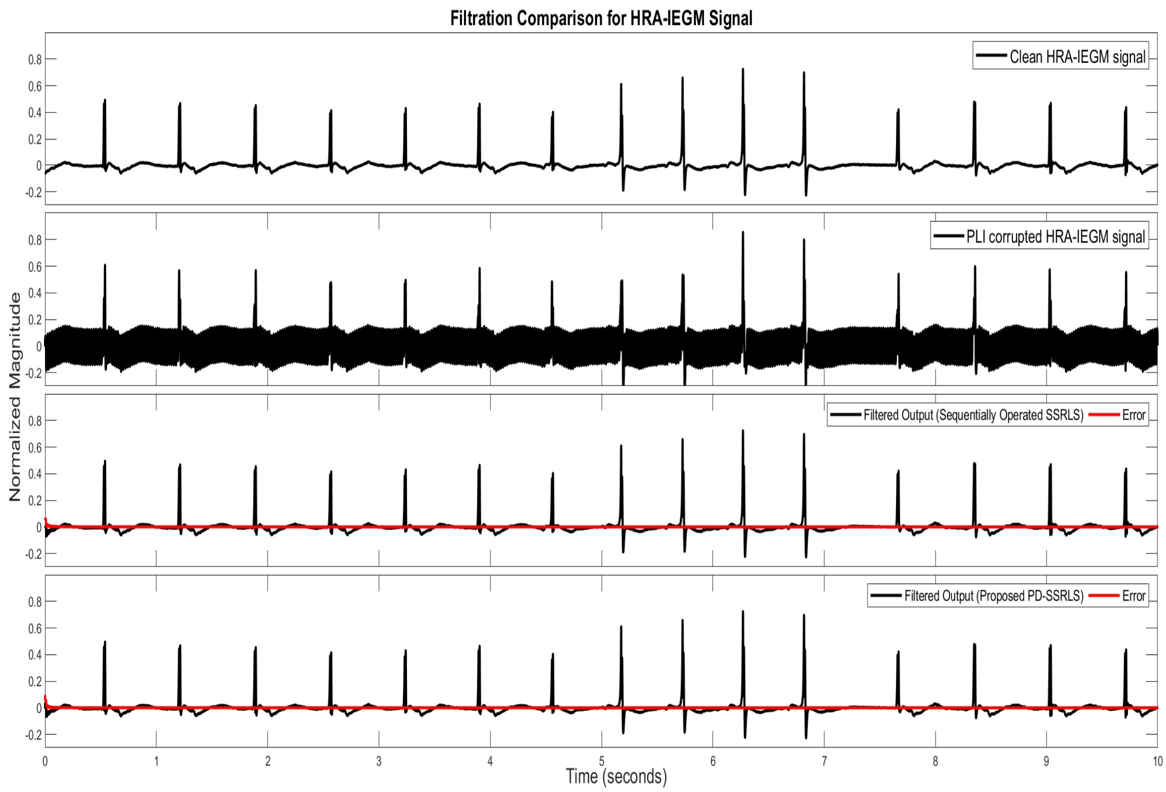


Fig. 9 Filtration comparison between Proposed PD-SSRLS and sequentially-operated SSRLS for HRA-IEGM signal

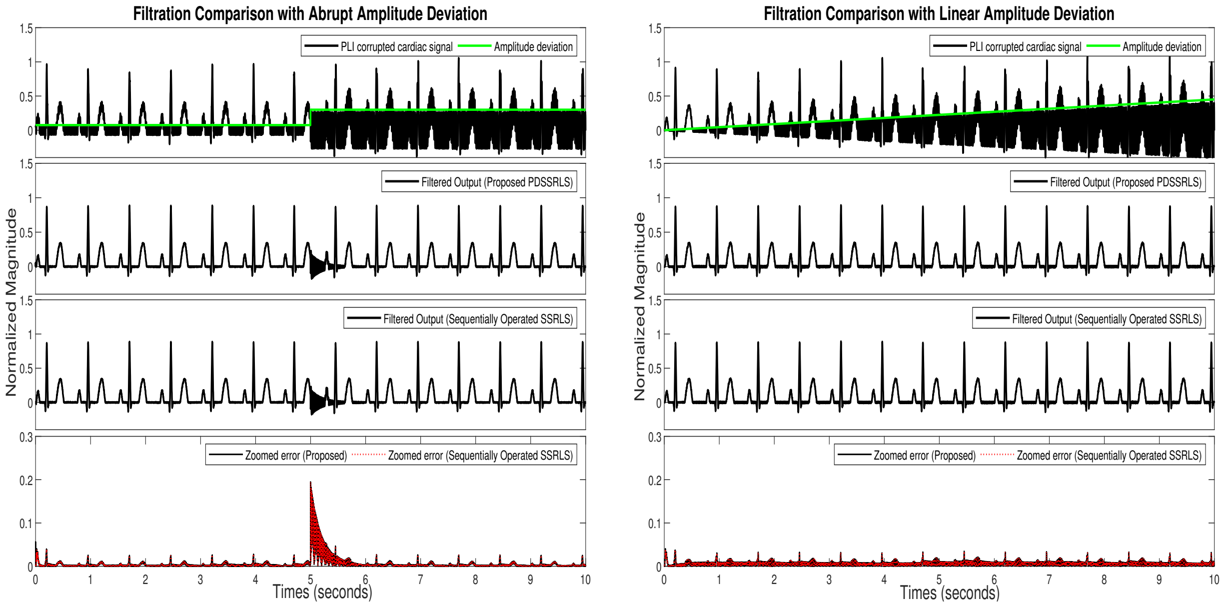


(a) Abrupt amplitude deviation (b) Linear amplitude deviation

Fig. 10 Filtration comparison of proposed PD-SSRLS and sequentially-operated SSRLS algorithm with abrupt and linear change in amplitude of PLI signal

The state space adaptive filter tracks the amplitude of PLI signal based on given frequency therefore, to estimate the change in frequency, the intelligent DFT (IDFT) technique mentioned in [32] is applied. The abrupt and linear change in frequency of PLI based corrupted cardiac signals are shown in Fig. 11. In Fig. 11(a) it can be realized that both the proposed PD-SSRLS and sequentially-operated SSRLS algorithms take approximately one second to adaptively track the abrupt frequency deviation. This extra 500 ms delay is because of the time taken by IDFT to estimate the frequency of PLI signal. Furthermore, the tracking performance of proposed PD-SSRLS adaptive filter in term of linear change in frequency of PLI signal is also the same than that of sequentially-operated SSRLS algorithm which is clearly depicted in Fig. 11(b).

The PLI based contaminated cardiac signal having both abrupt change in amplitude and frequency at different time instances is presented in Fig. 12. The zoomed error clearly depicts that the proposed PD-SSRLS provides almost the same convergence performance as compared to sequentially-operated SSRLS algorithm.

### *Quantitative performance*

In this section, the proposed PD-SSRLS technique is compared with that of sequentially operated SSRLS adaptive filter and subtraction procedure in terms of suppression ratio, correlation coefficient factor, the output SNR and MSE.

The performance criteria of the suppression ratio $\gamma$ with respect to various SNR values is compared in Fig. 13. It can be analyzed that the proposed PD-SSRLS algorithm has the same suppression ratio as of sequentially operated SSRLS.

In case of critical cardiac diseases like SCD, e-DYS and HRV, the shape or pattern of cardiac signal helps the cardiologist in clinical prognosis and diagnosis. Therefore, to measure the shape distortion due to PLI interference the correlation coefficient provided by the proposed PD-SSRLS and sequentially-operated SSRLS algorithm are compared in Fig. 14. It is observed

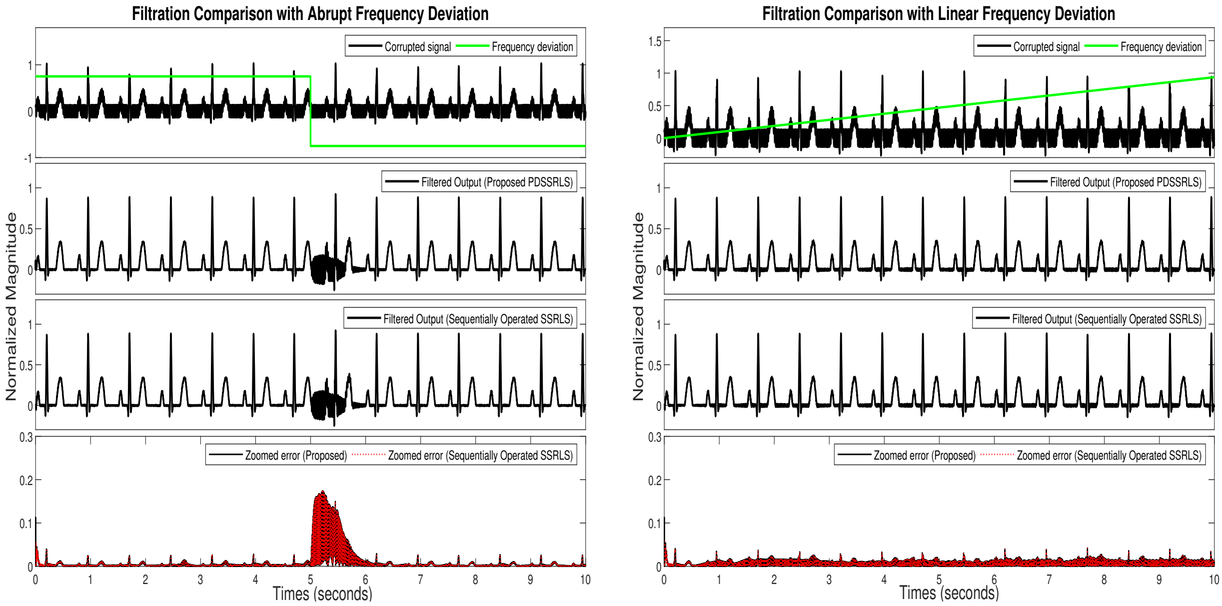


(a) Abrupt frequency deviation (b) Linear frequency deviation

Fig. 11 Filtration comparison of proposed PD-SSRLS and sequentially-operated SSRLS algorithm with abrupt and linear change in frequency of PLI signal

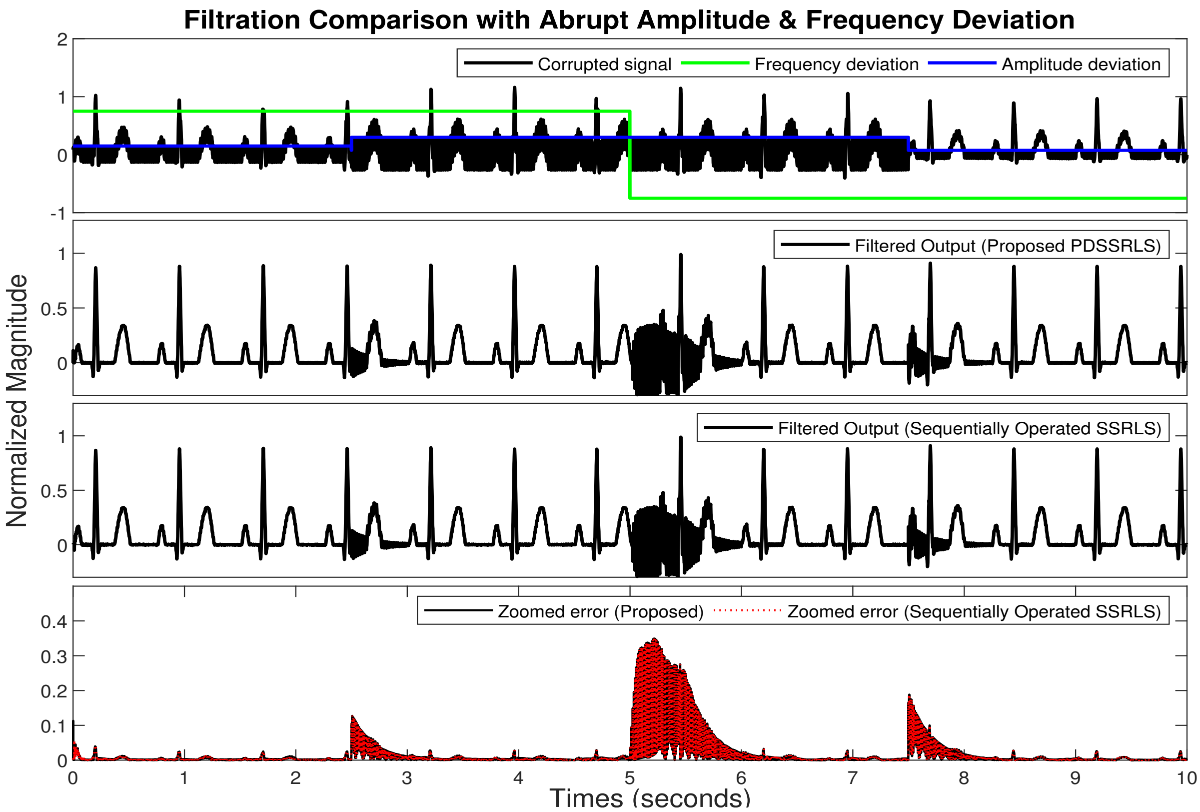


Fig. 12 Filtration comparison of proposed PD-SSRLS and sequentially-operated SSRLS algorithm with both abrupt change in amplitude and frequency of PLI

that the proposed architecture has almost negligible impact in term of shape distortion, while the overall correlation coefficient factor of SSRLS adaptive filter for PLI removal is very high even when the corrupted HRECG has a input SNR of –25dB.

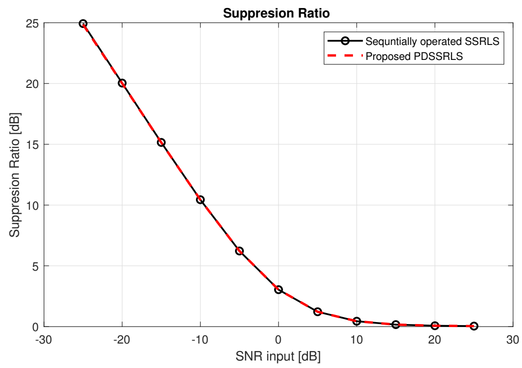


Fig. 13 Suppression ratio

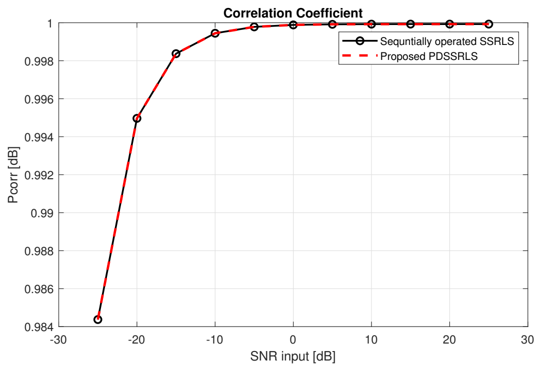


Fig. 14 Correlation coefficient

Furthermore, the comparison between the proposed PD-SSRLS and sequentially operated SS-RLS approach for output SNR and MSE are shown in Fig. 15 and Fig. 16, respectively. It can be seen that the output SNR and MSE provided by proposed PD-SSRLS architecture is slightly less than that of sequentially operated SSRLS algorithm. To operate the SSRLS algorithm in parallel fashion on individual platforms with different clock system is by putting the time as nonaligned [17]. Therefore, due to time nonaligned indexes, the performance in terms of output SNR and MSE of proposed PD-SSRLS is slightly less than that of sequentially operated SSRLS adaptive algorithm.

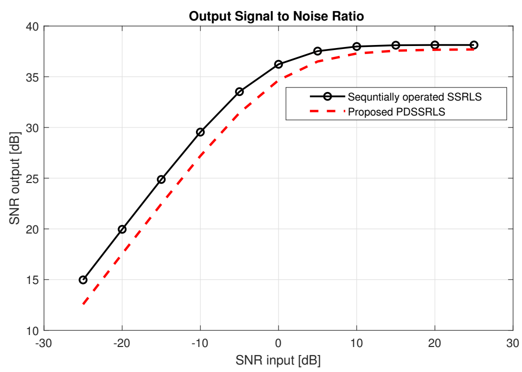


Fig. 15 Output SNR

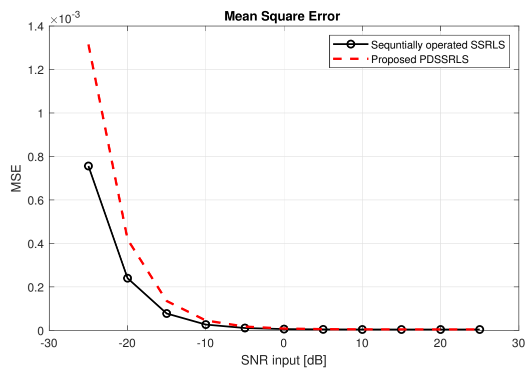


Fig. 16 Mean square error

The quantitative performance of proposed PD-SSRLS algorithm in terms of suppression ratio, correlation coefficient factor, the output SNR and MSE is almost same as that of sequentially-operated SSRLS for various input SNR. Furthermore, the statistical analysis has been drawn between the proposed PD-SSRLS algorithm and sequentially-operated SSRLS algorithm in terms of performance parameters on large dataset of different types of cardiac signal. The dataset includes 81 recordings of HRECG signal, 360 recordings UHF-ECG signal and 22 recordings of IEGM signal. The results clearly depicts that the proposed PD-SSRLS algorithm has almost the same quantitative performance in terms of suppression ratio, correlation coefficient factor, the output SNR and MSE as shown in Figs. 17-20, respectively.

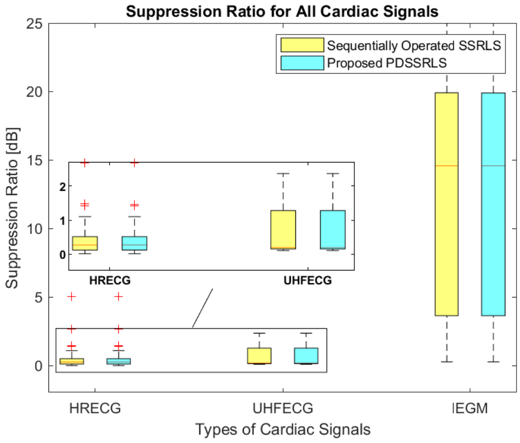


Fig. 17 Statistical analysis of suppression ratio

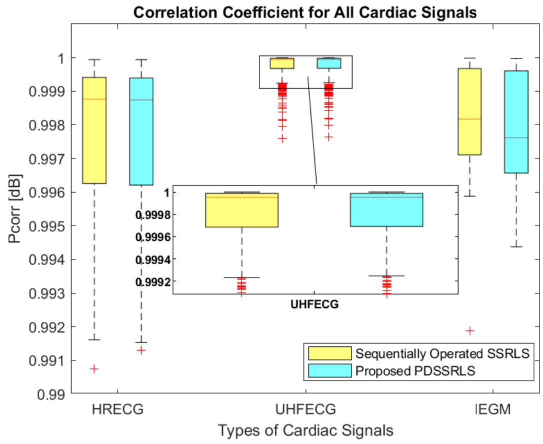


Fig. 18 Statistical analysis of correlation coefficient

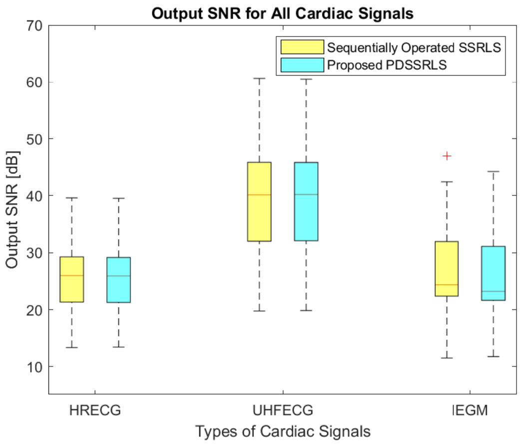


Fig. 19 Statistical analysis of output SNR

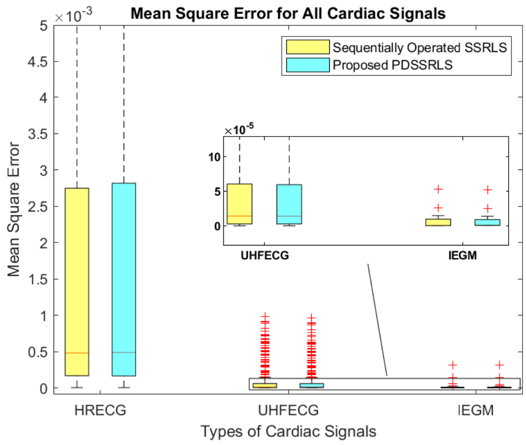


Fig. 20 Statistical analysis of MSE

## Conclusion

In this paper, a processing efficient distributed framework has been proposed which runs the computationally expensive state space recursive least square (SSRLS) adaptive algorithm parallely. The proposed parallel distributed SSRLS (PD-SSRLS) efficiently removes the PLI along with its harmonics even the time alignment among the contributing nodes is not the same. The proposed PD-SSRLS technique has been compared with that of sequentially operated SSRLS in terms of computational cost, convergence performance. The simulation results show that the proposed PD-SSRLS architecture provides less computational cost as compared to sequentially operated SSRLS algorithm. Furthermore, it has been observed that the qualitative and quantitative analysis of proposed PD-SSRLS exhibits nearly identical the performance to preserve the underlying cardiac activity as compared to sequentially operated SSRLS adaptive filter.


## Acknowledgements

*The authors are grateful to Dr. Pavel Jurak (Institute of Scientific Instruments of the Czech Academy of Sciences, Brno, Czech Republic) and National Institute of Heart Diseases (NIHD), Pakistan for providing the UHF-ECG, HRECG and IEGM cardiac signal samples, respectively.*

## References

1. Agrawal S., A. Gupta (2013). Fractal and EMD Based Removal of Baseline Wander and Powerline Interference from ECG Signals, Computers in Biology and Medicine, 43(11), 1889-1899.
2. Badreldin I. S., D. S. El-Kholy, A. A. El-Wakil (2010). A Modified Adaptive Noise Canceler for Electrocardiography with No Power-line Reference, Proceedings of the 5th Cairo International Biomedical Engineering Conference, 13-16.
3. Badreldin I. S., D. S. El-Kholy, A. A. Elwakil (2012). Harmonic Adaptive Noise Canceler for Electrocardiography with No Power-line Reference, Proceedings of the 16th IEEE Mediterranean Electrotechnical Conference, 1017-1020.
4. Bahaz M., R. Benzid (2018). Efficient Algorithm for Baseline Wander and Powerline Noise Removal from ECG Signals based on Discrete Fourier Series, Australasian Physical & Engineering Sciences in Medicine, 41(1), 143-160.
5. Bruce E. N. (2001). Biomedical Signal Processing and Signal Modeling, Wiley, New York.
6. Chavan M. S., R. Agarwala, M. Uplane (2008). Suppression of Baseline Wander and Power Line Interference in ECG Using Digital IIR Filter, International Journal of Circuits, Systems and Signal Processing, 2(2), 356-365.
7. De La Rosa F. (2006). Harmonics and Power Systems, CRC Press Boca Raton.
8. De Luna A. B. (2008). Basic Electrocardiography: Normal and Abnormal ECG Patterns, John Wiley & Sons.
9. Glover J. (1977). Adaptive Noise Canceling Applied to Sinusoidal Interferences, IEEE Transactions on Acoustics, Speech, and Signal Processing, 25(6), 484-491.
10. Graschew G., T. A. Roelofs, S. Rakowsky, P. M. Schlag (2011). Real-time Interactive Telemedicine for Ubiquitous Healthcare: Networks, Services and Scenarios, Advances in Telemedicine: Technologies, Enabling Factors and Scenarios, In Advances in Telemedicine: Technologies, Enabling Factors and Scenarios, Graschew G., T. A. Roelofs, (Eds.), InTechOpen.
11. Guleria R., R. Kaur (2016). Removing the Power Line Interference from ECG Signal Using Kalman Least Mean Square Filter, Proceedings of the International Conference on Signal Processing, Communication, Power and Embedded System (SCOPES), 1151-1157.
12. Haykin S. S. (2005). Adaptive Filter Theory, Pearson Education India.
13. Jiao Y., R. Y. Cheung, M. P. Mok (2012). Modified log-LMS Adaptive Filter with Low Signal Distortion for Biomedical Applications, Proceedings of the Annual International Conference of the IEEE Engineering in Medicine and Biology Society, 5210-5213.
14. Jain P., R. B. Pachori (2015). An Iterative Approach for Decomposition of Multicomponent Non-stationary Signals Based on Eigenvalue Decomposition of the Hankel Matrix, Journal of the Franklin Institute, 352(10), 4017-4044.
15. Jurak P., J. Halamek, J. Meluzin, F. Plesinger, T. Postranecka, J. Lipoldova, M. Novak, V. Vondra, I. Viscor, L. Soukup, P. Klimes, P. Vesely, J. Sumbera, K. Zeman, R. S. Asirvatham, J. Tri, S. J. Asirvatham, P. Leinveber (2017). Ventricular Dyssynchrony Assessment Using Ultra-high Frequency ECG Technique, Journal of Interventional Cardiac Electrophysiology, 49(3), 245-254.
16. Jurak P., K. Curila, P. Leinveber, F. W. Prinzen, I. Viscor, F. Plesinger, R. Smisek, R. Prochazkova, P. Osmancik, J. Halamek, M. Matejkova, J. Lipoldova, M. Novak, R. Panovsky, P. Andrla, V. Vondra, P. Stros, J. Vesela, D. Herman (2019). Novel Ultra-high-frequency Electrocardiogram Tool for the Description of the Ventricular Depolarization Pattern Before and During Cardiac Resynchronization, Journal of Cardiovascular Electrophysiology, 31(1), 300-307.

17. Khan N. M., H. Raza (2017). Processing-efficient Distributed Adaptive RLS Filtering for Computationally Constrained Platforms, Wireless Communications and Mobile Computing, 2017, Article ID 1248796.
18. Koseeyaporn P., J. Koseeyaporn, P. Wardkein (2009). An Enhanced Adaptive Algorithm for PLI Cancellation in ECG Signals, Proceedings of the 7th International Conference on Information, Communications and Signal Processing (ICICS), doi: 10.1109/ICICS.2009.5397681.
19. Kumar A., R. Ranganatham, R. Komaragiri, M. Kumar (2019). Efficient QRS Complex Detection Algorithm Based on Fast Fourier Transform, Biomedical Engineering Letters, 9(1), 145-151.
20. Levkov C., G. Mihov, R. Ivanov, I. Daskalov, I. Christov, I. Dotsinsky (2005). Removal of Power-line Interference from the ECG: A Review of the Subtraction Procedure, BioMedical Engineering OnLine, 4(1), 50.
21. Liu H., Y. Li, Y. Zhou, X. Jing, T.-K. Truong (2018). Joint Power Line Interference Suppression and ECG Signal Recovery in Transform Domains, Biomedical Signal Processing and Control, 44, 58-66.
22. Malik M. B. (2004). State-space Recursive Least-squares: Part I, Signal Processing, 84(9), 1709-1718.
23. Martens S. M., M. Mischi, S. G. Oei, J. W. Bergmans (2006). An Improved Adaptive Power Line Interference Canceller for Electrocardiography, IEEE Transactions on Biomedical Engineering, 53(11), 2220-2231.
24. Martis R. J., U. R. Acharya, L. C. Min (2013). ECG Beat Classification Using PCA, LDA, ICA and Discrete Wavelet Transform, Biomedical Signal Processing and Control, 8(5), 437-448.
25. Mihov G. (2018). Subtraction Procedure for Power-line Interference Removal from ECG Signals with High Sampling Rate, International Journal Bioautomation, 22(2), 147-158.
26. Mihov G. S., D. H. Badarov (2017). Testing of Digital Filters for Power-line Interference Removal from ECG Signals, Proceedings of the XXVI International Scientific Conference Electronics (ET), doi: 10.1109/ET.2017.8124368.
27. Narayanaswamy S. (2002). High Resolution Electrocardiography, Indian Pacing and Electrophysiology Journal, 2(2), 50-56.
28. Pei S.-C., C.-C. Tseng (1995). Elimination of AC Interference in Electrocardiogram Using IIR Notch Filter with Transient Suppression, IEEE Transactions on Biomedical Engineering, 42(11), 1128-1132.
29. Piskorowski J. (2012). Powerline Interference Removal from ECG Signal Using Notch Filter with Non-zero Initial Conditions, Proceedings of the IEEE International Symposium on Medical Measurements and Applications Proceedings, doi: 10.1109/MeMeA.2012.6226635.
30. Rakshit M., S. Das (2017). An Improved EMD based ECG Denoising Method Using Adaptive Switching Mean Filter, Proceedings of the 4th International Conference on Signal Processing and Integrated Networks (SPIN), 251-255.
31. Razzaq N., M. Butt, M. Salman, R. Ali, I. Sadiq, K. Munawar, T. Zaidi (2013). An Intelligent Adaptive Filter for Fast Tracking and Elimination of Power line Interference from ECG Signal, Proceedings of the 26th IEEE International Symposium on Computer-based Medical Systems, 251-256.
32. Razzaq N., S.-A. A. Sheikh, M. Salman, T. Zaidi (2016). An Intelligent Adaptive Filter for Elimination of Power Line Interference from High Resolution Electrocardiogram, IEEE Access, 4, 1676-1688.
33. Satija U., B. Ramkumar, M. S. Manikandan (2016). Low-complexity Detection and Classification of ECG Noises for Automated ECG Analysis System, Proceedings of the

IEEE International Conference on Signal Processing and Communications (SPCOM), doi: 10.1109/SPCOM.2016.7746621.

34. Shaik B. S., V. K. Chakka, S. Goli, A. S. Reddy (2016). Removal of Narrowband Interference (PLI in ECG Signal) Using Ramanujan Periodic Transform (RPT), Proceedings of the IEEE International Conference on Signal Processing and Communication (ICSC), 233-237.
35. Sharma R. R., R. B. Pachori (2018). Baseline Wander and Power Line Interference Removal from ECG Signals Using Eigenvalue Decomposition, Biomedical Signal Processing and Control, 45, 33-49.
36. Shin H. S., C. Lee, M. Lee (2010). Ideal Filtering Approach on DCT Domain for Biomedical Signals: Index Blocked DCT Filtering Method (IB-DCTFM), Journal of Medical Systems, 34(4), 741-753.
37. Singh P. (2016). Some Studies on a Generalized Fourier Expansion for Nonlinear and Nonstationary Time Series Analysis, Ph.D. Thesis, IIT Delhi, India.
38. Singh P., P. K. Srivastava, R. K. Patney, S. D. Joshi, K. Saha (2013). Nonpolynomial Spline Based Empirical Mode Decomposition, Proceedings of the IEEE International Conference on Signal Processing and Communication (ICSC), 435-440.
39. Singh P., S. D. Joshi, R. K. Patney, K. Saha (2017). The Fourier Decomposition Method for Nonlinear and Non-stationary Time Series Analysis, Proceedings of the Royal Society A: Mathematical, Physical and Engineering Sciences, 473, 20160871.
40. Singhal A., P. Singh, B. Fatimah, R. B. Pachori (2020). An Efficient Removal of Powerline Interference and Baseline Wander from ECG Signals by Employing Fourier Decomposition Technique, Biomedical Signal Processing and Control, 57, 101741.
41. Soedirdjo S. D., K. Ullah, R. Merletti (2015). Power Line Interference Attenuation in Multi-channel sEMG Signals: Algorithms and Analysis, Proceedings of the 37th Annual International Conference of the IEEE Engineering in Medicine and Biology Society (EMBC), IEEE, 3823-3826.
42. Thomas C. W., W. P. Huebner, R. J. Leigh (1988). A Low-pass Notch Filter for Bioelectric Signals, IEEE Transactions on Biomedical Engineering, 35(6), 496-498.
43. Van Alste J. A., T. Schilder (1985). Removal of Base-line Wander and Power-line Interference from the ECG by an Efficient Fir Filter with a Reduced Number of Taps, IEEE Transactions on Biomedical Engineering, 12, 1052-1060.
44. Wang J., Y. Ye, X. Pan, X. Gao, C. Zhuang (2014). Fractional Zero-phase Filtering Based on the Riemann-Liouville Integral, Signal Processing, 98, 150-157.
45. Widrow B., J. R. Glover, J. M. McCool, J. Kaunitz, C. S. Williams, R. H. Hearn, J. R. Zeidler, J. E. Dong, R. C. Goodlin (1975). Adaptive Noise Cancelling: Principles and Applications, Proceedings of the IEEE, 63(12), 1692-1716.

 doi: 10.7546/ijba.2021.25.3.000781

**Inam ur Rehman, Ph.D. Student**
E-mail: muhammad.inam@ceme.nust.edu.pk

Inam ur Rehman received the B.E. (Hons.) degree in Electronics Engineering from the Islamia Uiversity of Bahawalpur, Bahawalpur, Pakistan, in 2007, and the M.Sc. degree in Electrical Engineering from the College of Electrical and Mechanical Engineers, National University of Sciences and Technology, Islamabad, Pakistan, in 2011. He is currently pursuing the Ph.D. degree in Intracardiac Signals (Biomedical Engineering). His field of specialization is biomedical engineering and cardiac signal processing. He is a Life Time Member of the Pakistan Engineering Council.

**Assist. Prof. Hasan Raza, Ph.D.**
E-mail: hasan.raza@hamdard.edu.pk

Hasan Raza was born in Pakistan in 1988. He received both the B.Sc. and M.Sc. degrees in Electronics Engineering from Muhammad Ali Jinnah University, Pakistan, in 2010 and 2012, respectively. He is the M.Sc. (EE) gold medalist of the batch year, 2010. In 2019, he completed his Ph.D. degree in Electrical Engineering from Capital University of Science and Technology, Islamabad. Currently, he is working as an Assistant Professor with the Hamdard University, Islamabad, Pakistan. His research interests include adaptive signal processing, channel estimation, distributed estimation and information security.

**Assoc. Prof. Nauman Razzaq, Ph.D.**
E-mail: nauman.razzaq@nutech.edu.pk

Nauman Razzaq received the B.E. degree (with honors) in Electrical Engineering from the College of Electrical and Mechanical Engineering, Islamabad, Pakistan, in 1995. He received his M.Sc. degree in Electrical Engineering from UET, Peshawar, Pakistan, in 2004. He completed his Ph.D. degree in the field of Biomedical (Electrical) Engineering from College of Electrical and Mechanical Engineering, National University of Science and Technology, Islamabad, Pakistan in 2017. His field of specialization is biomedical engineering and cardiac signal processing. He has a vast experience as professional biomedical engineer of serving in Armed Forces Institute of Cardiology National Institute of Heart Diseases, Pakistan. He holds the position of an Associate Professor and serves as Head of Electrical Engineering Department at National University of Technology, Islamabad, Pakistan. He is a Life Time Member of the Pakistan Engineering Council.

**Assoc. Prof. Tahir Zaidi, Ph.D.**
E-mail: tahirzaidi@ceme.nust.edu.pk

Tahir Zaidi received the M.Sc. degree in Computer Engineering from the Center for Advanced Studies in Engineering, Pakistan, and the Ph.D. degree from Georgia Tech, USA. He is currently an Associate Professor with the Department of Electrical Engineering, College of Electrical and Mechanical Engineering, National University of Science and Technology, Pakistan. He has extensive experience in the area of biomedical equipment and presently working on multiple collaborative projects with the Armed Institute of Cardiology and Shifa International Hospitals. His team has successfully developed high resolution ECG, Holter monitor, and intracardiac signal acquisition analysis and display system. He was a Gold Medalist from the College of Aeronautical Engineering, Pakistan, in 1990.